Available online at www.sciencedirect.com
ScienceDirect
International Journal of Heat and Mass Transfer 50 (2007) 5161–5167
International Journal of HEAT and MASS TRANSFER
www.elsevier.com/locate/ijhmt

Analytical modeling of electrokinetic effects on flow and heat transfer in microchannels

Abhishek Jain, Michael K. Jensen *

Department of Mechanical, Aerospace and Nuclear Engineering, Rensselaer Polytechnic Institute, Troy, NY 12180, USA

Received 27 June 2007
Available online 11 September 2007

Abstract

A fundamental understanding of electrolytic flow in microchannels is essential for the design of microfluidic devices. Hence, an analytic investigation is presented on the effects of electrostatic potential in microchannels. Solving the Navier–Stokes equations, an expression for the $C_f Re$ product is presented. Solving the energy equation the Nusselt number for constant wall heat flux and constant wall temperature boundary conditions are presented with analytic expressions over a wide range of operating conditions.

Keywords: Electric double layer; Electro-viscous effect; Friction factor; Nusselt number

1. Introduction

Micro-electro-mechanical-systems (MEMS) and other microfluidic technologies have revolutionized many aspects of applied sciences and engineering, such as heat exchangers [1], pumps [2], combustors, gas absorbers, solvent extractors, fuel processors [3], and on-chip biomedical and biochemical analysis instruments [4]. All of these devices involve fluid flow and heat transfer in microchannels. Indeed, much study has been focused on microchannels [5] for efficient cooling of chips due to their very high heat transfer coefficients [6].

When dealing with micro-fluidics or flows in microchannels, the interfacial effects (phenomenon happening at the surface of the microchannel), which are negligible in bulk fluid flows, becomes more pronounced [7–13]. In particular, electrolytic flow in microchannels can be significantly different than non-electrolytic flows. The phenomenon manifests itself by generating a viscous effect, which affects both the flow and heat transfer.

The present work deals with the modification of Navier–Stokes equation to take into account the effect of electrokinetics and the development of analytic expressions for both the friction factor and Nusselt number. Previous investigations have ignored these effects at lower ionic concentrations. The present work is applicable over the complete range of ionic concentration.

2. Governing equations

While the application is for flow in microchannels that have rectangular or trapezoidal cross- section, the present analysis is applied to an infinite parallel plate channel. To apply the governing Navier–Stokes and energy equations to this situation, the following simplifying assumptions are made:

1. The flow is laminar, incompressible, steady, fully developed hydrodynamically and thermally, and the channel is considered as infinite parallel plates.
2. Gravity forces are ignored.
3. The fluid is Newtonian and its properties are independent of the local electric field strength.
4. The ions are point charges, with no concentration gradients in the flow.
5. Zeta potential is assumed to be uniform over the surface.

* Corresponding author. Tel.: +1 518 276 2843; fax: +1 518 276 6025.
E-mail address: JenseM@rpi.edu (M.K. Jensen).

0017-9310/$ - see front matter © 2007 Elsevier Ltd. All rights reserved.
doi:10.1016/j.ijheatmasstransfer.2007.07.005

6. Viscous dissipation is neglected as its magnitude is very small in microchannel flows and the pressure force is the dominating factor.
7. The fluid is a continuum, and the Knudsen number is <0.1.

Application of these assumptions to the three governing equations results in:
Continuity equation:

$$\frac{du}{dx} = 0 \tag{1}$$

Navier–Stokes equation:

$$\mu\frac{d^2u}{dy^2} - \frac{dp}{dx} + \rho_e E_x = 0 \tag{2}$$

Energy equation:

$$u\frac{dT}{dx} = \alpha\left(\frac{\partial^2 T}{\partial y^2}\right) \tag{3}$$

where x is the direction along the flow and y is the direction perpendicular to fluid flow and is measured from the channel centerline. The forces acting on an element of liquid include the pressure force, the viscous force and the electrical body force generated by the flow-induced electro-kinetic field (i.e., the streaming potential) represented by the term $\rho_e E_x$, where ρ_e is the net charge density per unit volume and E_x is the non-dimensional streaming electric field. We must develop an expression for $\rho_e E_x$ before the above equations can be solved.

2.1. Development of surface charges and electric double layer

Any surface is likely to carry some charges because of "broken bonds" and "surface charge traps". Likewise, most surfaces acquire an electrostatic charge when in contact with an aqueous solution. If the liquid contains a very small amount of ions (due to impurities), the presence of a surface charge causes both counter-ions and co-ions in the liquid to be preferentially redistributed, leading to the formation of the electric double layer (EDL) near the wall.

The EDL can be divided into an *inner compact layer* and an *outer diffuse layer*. Ions of opposite charges cluster close to the wall, forming the Stern layer or the Shear Plane, and the ions within the Stern layer are attracted to the wall with very strong electrostatic forces. The wall electrostatic attraction causes the counter-ion concentration to be higher near the solid surface as compared to the bulk fluid away from the wall. Contrary to this the co-ion concentration near the surface is lower than that in the bulk liquid, due to the electrostatic repulsion. In contrast, ions in the diffuse layer are less affected by the charged surface (than those in the compact or inner layer) and, hence, are mobile. The thickness of the diffuse layer is dependent on the bulk ionic concentration and electrical properties of the liquid. Electrostatic potential is generally measured at the shear plane, where the electric potential is measurable and is called the *zeta potential*, denoted by ζ, which typically decays exponentially at distances farther from the wall.

The fluid flow in the microchannel results in the downstream flow of the counter-ions. This causes an electric current, called the streaming current, in the direction of fluid flow. The streaming potential associated with the streaming current is called electro-kinetic potential. This potential drives the counter-ions in the direction opposite to the streaming current. When the ions move in the liquid, they exert a force on the liquid molecules, thus generating a viscous effect, usually referred to as the electro-viscous effect. Generally, for macrochannel flow the EDL effects can be safely neglected, as the thickness of the EDL is very small compared with the hydraulic diameter of the channels. However, for microchannel flow the thickness of the EDL is often comparable with the characteristic size of the channels and cannot be neglected.

2.2. Poisson–Boltzmann equation

The electrostatic potential ψ is related to the local net charge density per unit volume ρ_e at certain points in the solution by the Poisson equation as:

$$\frac{d^2\psi}{dy^2} = -\frac{\rho_e}{\varepsilon} \tag{4}$$

where ε is the permittivity or the dielectric constant of the solution. Assuming that the equilibrium Boltzmann distribution equation is applicable, the number concentration of the type-i ions, denoted by n_i, in a symmetric electrolyte solution is of the form:

$$n_i = n_{io}\exp\left(-\frac{z_i e\psi}{k_B T}\right) \tag{5}$$

where n_{io} and z_i are bulk ionic concentration and the valence of type-i ions, respectively, e is the charge of an electron, k_B is the Boltzmann constant and T is the absolute temperature.

For a symmetric electrolyte of valence z, the net volume charge density ρ_e is related to the total concentration difference between the cations and anions as:

$$\rho_e = ze(n_+ - n_-) \tag{6}$$

Substituting the values of the number concentration of each ion from Eq. (5) into Eq. (6), we obtain:

$$\rho_e = -2zen_o\sinh\left(\frac{ze\psi}{k_B T}\right) \tag{7}$$

where n_o is the bulk ion concentration of each ion.

Substituting the value of charge density (Eq. (7)) in the Poisson equation (Eq. (4)) results in:

$$\frac{d^2\psi}{dy^2} = \frac{2zen_o}{\varepsilon}\sinh\left(\frac{ze\psi}{k_B T}\right) \tag{8}$$

The above non-linear second-order one-dimensional equation is known as the Poisson–Boltzmann equation.

Now we define the non-dimensional transverse coordinate $\bar{y}$, the non-dimensional electric potential $\bar{\psi}$, the Debye–Hückel parameter, k, and the electrokinetic distance κ as:

$$\bar{y} = \frac{y}{a}, \quad \bar{\psi} = \frac{ze\psi}{k_B T}, \quad k^2 = \frac{2z^2 e^2 n_o}{\varepsilon k_B T} \quad \text{and} \quad \kappa = ka$$

where $2a$ is the width of the microchannel. Using these definitions we obtain the governing equation:

$$\frac{d^2\bar{\psi}}{d\bar{y}^2} = \kappa^2 \sinh(\bar{\psi}) = -\frac{\kappa^2}{2}\bar{\rho} \tag{9}$$

where $\bar{\rho} = -2\sinh(\bar{\psi})$.

2.3. Debye–Hückel linear approximation

The Debye–Hückel parameter k is independent of the solid-surface properties and is determined by the liquid properties only. $1/k$ is referred to as the '*characteristic thickness*' of the EDL. k can be modified to take into account the ionic strength or the molarity (number of moles of the solute per unit volume) of the solution.

If the electrical potential is small compared to the thermal energy of the ions, i.e., ($|ze\psi| < |k_B T|$) so that the sine function in Eq. (9) can be approximated by $\sinh\bar{\psi} \approx \bar{\psi}$, then the equation transforms into:

$$\frac{d^2\bar{\psi}}{d\bar{y}^2} = \kappa^2\bar{\psi} \tag{10}$$

This treatment is usually called the Debye–Hückel linear approximation [14]. At small electrolyte concentrations [15], the Debye–Hückel approximation is good, and the solution to Eq. (10) is given by:

$$\bar{\psi} = c_1 e^{\kappa\bar{y}} + c_2 e^{-\kappa\bar{y}}$$

Applying boundary conditions:

$$\text{At } \bar{y} = 0, \ \frac{d\bar{\psi}}{d\bar{y}} = 0 \quad \text{and} \quad \text{at } \bar{y} = 1, \ \bar{\psi} = \bar{\zeta}$$

i.e., at the center of the microchannel there is no potential gradient and at the walls (actually near the shear plane), the potential is equivalent to $\bar{\zeta}$ defined as:

$$\bar{\zeta} = \frac{ze\zeta}{k_B T} \tag{11}$$

Applying the above boundary conditions we get

$$\bar{\psi} = \frac{\bar{\zeta}}{\sinh(\kappa)}\sinh(\kappa\bar{y}) \tag{12}$$

Increasing the parameter κ, the potential is oriented towards the wall region as more and more ions adhere to the wall. However, if the value of the zeta potential increases, the value of streaming potential increases and also moves away from the wall. This happens because an increased zeta potential implies an increase in the relative charge density of the ions near the wall which, in turn, produces a relatively higher magnitude of the potential, the presence of which can be felt in a region farther from the wall.

3. Solution of the governing equations

Using the following non-dimensional parameters:

$$\bar{u} = \frac{u}{U}, \quad \bar{y} = \frac{y}{a}, \quad \bar{\rho} = \frac{\rho_e}{n_0 ze}, \quad E_x = \frac{E_s}{L}, \quad \overline{E}_s = \frac{E_s}{\zeta_o}$$

where U is the average velocity for Poiseuille flow, E_s is the streaming potential, E_x is the non-dimensional streaming electric field, L is the length of the micro-channel and ζ_o is the potential at the center of the channel, we can rewrite the governing equations.

From Eq. (9), we can write

$$\bar{\rho} = -\frac{2}{\kappa^2}\frac{d^2\bar{\psi}}{d\bar{y}^2} \tag{13}$$

Substituting the non-dimensional terms into Eq. (2) and rearranging, we get:

$$\frac{d^2\bar{u}}{d\bar{y}^2} - \frac{a^2}{\mu U}\frac{dp}{dx} - \frac{2}{\kappa^2}\frac{n_o zea^2\zeta_o}{\mu UL}\overline{E}_s\frac{d^2\bar{\psi}}{d\bar{y}^2} = 0$$

The above equation can be written as:

$$\frac{d^2\bar{u}}{d\bar{y}^2} + \Gamma_1 - \frac{2\Gamma_2\overline{E}_s}{\kappa^2}\frac{d^2\bar{\psi}}{d\bar{y}^2} = 0 \tag{14}$$

where Γ_1 and Γ_2 are given by:

$$\Gamma_1 = -\frac{a^2}{\mu U}\frac{dp}{dx} \quad \text{and} \quad \Gamma_2 = \frac{n_o zea^2\zeta_o}{\mu UL}$$

$2\overline{E}_s/\kappa^2$ is not incorporated into Γ_2 since Γ_2 allows the influence of the electrolytic properties to be seen to a greater extent. Also, $\overline{E}_s$ can be varied to study its effect on different parameters.

Solving Eq. (14) for the velocity profile, we get:

$$\bar{u} = -\frac{\Gamma_1\bar{y}^2}{2} + \frac{2\Gamma_2\overline{E}_s}{\kappa^2}\bar{\psi} + c_1\bar{y} + c_2 \tag{15}$$

Now applying the boundary conditions:

$$\text{At } \bar{y} = 0 : \frac{d\bar{\psi}}{d\bar{y}} = 0, \ \frac{d\bar{u}}{d\bar{y}} = 0 \quad \text{and} \quad \text{at } \bar{y} = 1 : \bar{\psi} = \bar{\zeta}, \ \bar{u} = 0$$

we get:

$$\bar{u} = \frac{\Gamma_1(1-\bar{y}^2)}{2} - \frac{2\Gamma_2\overline{E}_s\bar{\zeta}}{\kappa^2}\left(1 - \frac{\bar{\psi}}{\bar{\zeta}}\right)$$

Substituting the above boundary conditions into this equation and the value of $\bar{\psi}$ from Eq. (12), the velocity profile is obtained:

$$\bar{u} = \underbrace{\frac{\Gamma_1(1-\bar{y}^2)}{2}}_{\text{I}} - \underbrace{\frac{2\Gamma_2\overline{E}_s\bar{\zeta}}{\kappa^2}\left|\left(1 - \frac{\sinh(\kappa\bar{y})}{\sinh(\kappa)}\right)\right|}_{\text{II}}$$

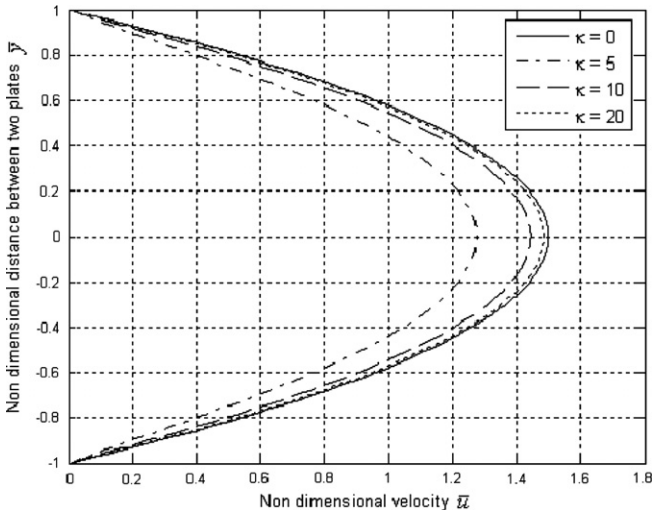

Fig. 1. Non-dimensional velocity distribution for various values of κ at $\bar{\zeta} = 1$.

Term I signifies the contribution of the applied pressure gradient, and term II represents the contribution of EDL to the velocity.

Fig. 1 shows the non-dimensional velocity profile for different sets of κ. As can be inferred from the equation, if there is no EDL (i.e., $\overline{E}_s = 0$ and $\bar{\zeta} = 0$ at $\kappa = 0$), then $\bar{u} = \frac{\Gamma_1}{2}(1 - \bar{y}^2)$, which is the conventional form of the Poiseuille flow velocity profile between two parallel plates. Thus, the effect of the EDL is to reduce the velocity of the flow; this, in turn, affects the heat transfer.

3.1. $C_f Re$ product

In the standard case for fluid flow between parallel plates the $C_f Re$ product is numerically equal to 24. Now from the definition of C_f

$$C_f = \frac{\tau_w}{\frac{1}{2}\rho U^2} = \frac{\mu \frac{\partial u}{\partial y}\Big|_{y=a}}{\frac{1}{2}\rho U^2}$$

and using the non-dimensional velocity profile, we get the following equation for the dependence of $C_f Re$ on zeta potential and non-dimensional parameter κ:

$$C_f Re = 24 + 16\Gamma_2 \overline{E}_s \bar{\zeta} \frac{\cosh(\kappa)}{\kappa \sinh(\kappa)} \tag{16}$$

where Reynolds number Re is defined as:

$$Re = \frac{\rho U(4a)}{\mu}$$

The $C_f Re$ product increases with increasing value of $\bar{\zeta}$ because with increase in zeta potential, the effect of the electrostatic potential near the wall dominates in regions near the wall and also away from the wall. This results in an apparent increase in the viscosity and, hence, the $C_f Re$ product increases.

Fig. 2 shows the variation of $C_f Re$ with κ at specified zeta potentials. The value of $C_f Re$ decreases with κ and approaches the conventional value of 24. The increase in the value of $C_f Re$ with zeta potential can be attributed to the fact that on increasing the value of zeta potential the presence of electric double layer can be felt in a region at a greater distance from the wall which enhances the viscosity, and hence, causes an increase in the value of $C_f Re$. Using the values of different parameters as listed below that comprise Γ_2 and $\overline{E}_s$ the value for the product of $\Gamma_2 \overline{E}_s$ is taken as 2.7107×10^{-4} for illustration purposes:

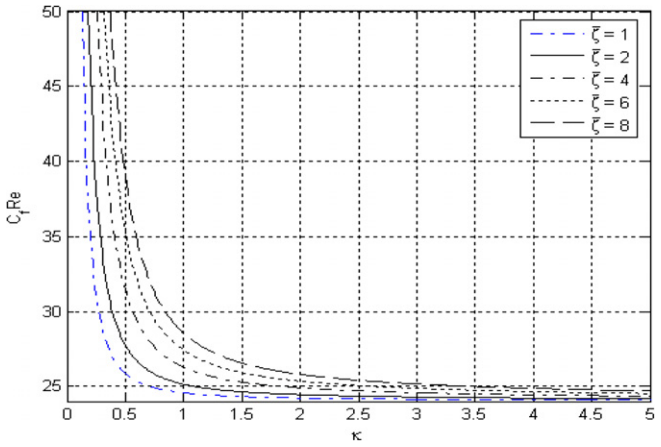

Fig. 2. $C_f Re$ variation with κ at specified $\bar{\zeta}$ [Eq. (16)].

$$a_0 = 5 \times 10^{-6}\ \text{m}, \quad n_0 = 6.023 \times 10^{23}, \quad U = 1\ \text{m/s},$$
$$e = 1.60219 \times 10^{-19}\ \text{C}, \quad \mu = 0.00089\ \text{kg/m-s},$$
$$\text{with } E_s = 100\ \text{mV}$$

Due to the asymptotic behavior at very low values of κ, it is difficult to use the expression given by Eq. (16) at these values and the equation developed is undefined at $\kappa = 0$. Hence, an approximation needs to be incorporated, which will take into account this problem and also to ensure the convergence of $C_f Re$ to the conventional value of 24 at $\kappa = 0$.

For very low values of κ the charge distribution is irregular. Moreover, the charges have negligible effect on the flow patterns; thereby, the flow remains more or less laminar. However, due to algebraic complexities the lower κ values give rise to an asymptotic behavior with $C_f Re \to \infty$ and, hence, needs to be rectified.

3.2. Approximation for $C_f Re$ at smaller values of κ

Solving for the electrostatic potential field using the following boundary conditions:

$$\text{At } y = 0, \ \frac{d\psi}{dy} = 0 \text{ and at } y = a, \ \psi = \zeta$$

we get:

$$\psi = \frac{\zeta}{(e^{ka} + e^{-ka})}(e^{ky} + e^{-ky})$$

Replacing the exponential series in the numerator with the hyperbolic cosine series without changing the exponential series in the denominator, substituting the electrostatic potential value given by the above equation into the momentum equation, and solving for the velocity profile we get the following expression for the dimensional velocity profile:

$$u = \frac{1}{2\mu}\frac{dP}{dx}(y^2 - a^2) + \frac{2\varepsilon E_x}{\mu}\frac{\zeta}{(e^{ka} + e^{-ka})}\{\cosh(ky) - \cosh(ka)\}$$

Now expanding the exponential series and taking only the first two terms as for lower values of ka the higher terms are negligible, hence, the term $(e^{ka} + e^{-ka})$ takes the value of 2. From the definition of C_f the final expression for $C_f Re$ is:

$$C_f Re = 24 + \frac{8\varepsilon k_B T}{z^2 e^2 a^2 n_0}\Gamma_2 \overline{E}_s \bar{\zeta}\kappa \sinh(\kappa)$$

Substituting the values of different parameters we get:

$$C_f Re = 24 + 6.029 \times 10^{-5}\Gamma_2 \overline{E}_s \bar{\zeta}\kappa \sinh(\kappa) \quad (17)$$

Combining Eqs. (16) and (17), we can obtain values of $C_f Re$ for the complete range of κ. Fig. 3 shows the variation of $C_f Re$ at different ionic concentrations. From the figure it is clear that when $\kappa = 0$, the respective product value converges to the conventional value of 24. On increasing the value of κ the product rises as a result of the small turbulence created by the ionic distribution. However, at larger values of κ the wall is completely surrounded by the counter-charges and there are fewer disturbances in the flow which decreases the $C_f Re$ product. As can be seen, for certain combinations of conditions, electrokinetic effects can have a large effect on flow.

3.3. Analysis of Nusselt number (constant heat flux)

Solving the energy equation, Eq. (3), using the non-dimensional temperature profile $\phi = \frac{T - T_s}{T_m - T_s}$, and incorporating an energy balance on a small segment of the channel, we get:

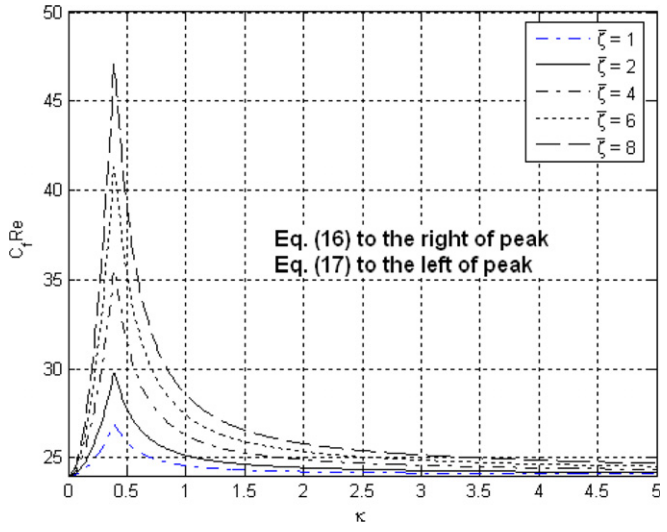

Fig. 3. $C_f Re$ variation for complete range of κ.

$$\frac{u}{\alpha}\frac{q''}{\rho U c_p a} = \frac{d^2 T}{dy^2} \quad (18)$$

where T_s and T_m are the surface and mean temperatures, respectively. Substituting the non-dimensional velocity profile into Eq. (18) and incorporating the non-dimensional temperature profile and non-dimensional distance $\bar{y}$, we get:

$$\left[\frac{3}{2}(1 - \bar{y}^2) - Z\left(1 - \frac{\sinh(\kappa\bar{y})}{\sinh(\kappa)}\right)\right]\frac{q''}{ka(T_m - T_s)} = \frac{1}{a^2}\frac{d^2\left(\frac{T - T_s}{T_m - T_s}\right)}{d\bar{y}^2} \quad (19)$$

where $Z = 2\Gamma_2 \overline{E}_s \bar{\zeta}/\kappa^2$.

Eq. (19) can be written as:

$$-\left[\frac{3}{2}(1 - \bar{y}^2) - Z\left(1 - \frac{\sinh(\kappa\bar{y})}{\sinh(\kappa)}\right)\right]\frac{h}{ka} = \frac{1}{a^2}\frac{d^2\phi}{d\bar{y}^2}$$

or

$$-\frac{Nu}{4}\left[\frac{3}{2}(1 - \bar{y}^2) - Z\left(1 - \frac{\sinh(\kappa\bar{y})}{\sinh(\kappa)}\right)\right] = \frac{d^2\phi}{d\bar{y}^2} \quad (20)$$

where Nusselt number is defined as: $Nu = (4a)h/k$. Integrating Eq. (20) twice to get an expression for the non-dimensional temperature profile:

$$\phi = -\frac{Nu}{4}\left[\frac{3}{2}\left(\frac{\bar{y}^2}{2} - \frac{\bar{y}^4}{12}\right) - Z\left(\frac{\bar{y}^2}{2} - \frac{\sinh(\kappa\bar{y})}{\kappa^2 \sinh(\kappa)}\right)\right] + c_1\bar{y} + c_2$$

Applying the boundary conditions:

$$\text{At } y = 0,\ \frac{\partial\phi}{\partial y} = 0 \quad \text{and} \quad \text{at } y = 1,\ \phi = 0$$

we obtain the following expression for the non-dimensional temperature profile:

$$\phi = -\frac{Nu}{4}\left[\frac{3}{2}\left(\frac{\bar{y}^2}{2} - \frac{\bar{y}^4}{12} - \frac{5}{12}\right)\right] + \frac{Nu}{4}\left[Z\left(\frac{\bar{y}^2}{2} - \frac{\sinh(\kappa\bar{y})}{\kappa^2 \sinh(\kappa)} + \frac{\bar{y}}{\kappa \sinh(\kappa)} - \frac{1}{2} + \frac{1}{\kappa^2} - \frac{1}{\kappa \sinh(\kappa)}\right)\right] \quad (21)$$

From the definition of mean temperature:

$$1 = \frac{1}{2}\int_{-1}^{1}\left(\frac{u}{U}\right)(\phi)\,d\bar{y}$$

Solving Eq. (21) for Nusselt number, we get the following expression:

$$Nu = \frac{8}{I} \quad (22)$$

where the term I is:

$$I = \int_{-1}^{1}\left[\frac{3}{2}(1 - \bar{y}^2) - Z\left(1 - \frac{\sinh(\kappa y)}{\sinh(\kappa)}\right)\right]\left[\frac{3}{2}\left(-\frac{\bar{y}^2}{2} + \frac{\bar{y}^4}{12} + \frac{5}{12}\right) + Z\Upsilon\right]d\bar{y}$$

and

$$\Upsilon = \left(\frac{\bar{y}^2}{2} - \frac{\sinh(\kappa y)}{\kappa^2 \sinh(\kappa)} + \frac{\bar{y}}{\kappa \sinh(\kappa)} - \frac{1}{2} + \frac{1}{\kappa^2} - \frac{1}{\kappa \sinh(\kappa)}\right)$$

As shown in Fig. 4, similar to the behavior pattern of $C_f Re$ product, the above equation tends to follow the asymptotic behavior at very low values of κ. To overcome the asymptotic behavior at lower values of κ the following methodology is adopted.

3.3.1. Approximation made at lower values of κ

From the non-dimensional momentum equation:

$$\frac{\mu U}{a^2}\frac{d^2\bar{u}}{dy^2} - \frac{dP}{dx} + \bar{\rho} z e n_0 \frac{\overline{E}_s \zeta_0}{L} = 0 \tag{23}$$

Substituting the value of the non-dimensional electric charge density ($\bar{\rho} = -2\sinh(\bar{\psi})$) into Eq. (23) and solving for the non-dimensional velocity profile:

$$\bar{u} = \frac{\Gamma_1}{2}(1-\bar{y}^2) + \Gamma_2 \overline{E}_s\left(\sinh(\bar{\psi})y^2 - \sinh(\bar{\zeta})\right)$$

Substituting this non-dimensional velocity profile into the energy equation we obtain the non-dimensional temperature profile:

$$\phi = \frac{Nu}{4}\left[\left(-\frac{\bar{y}^2}{2} + \frac{\bar{y}^4}{12} + \frac{5}{12}\right) + \Gamma_2 \overline{E}_s\left\{-\sinh(\bar{\psi})\frac{\bar{y}^4}{12} + \sinh(\bar{\zeta})\frac{\bar{y}^2}{2} + \sinh(\bar{\psi})\frac{1}{12} - \sinh(\bar{\zeta})\frac{1}{2}\right\}\right]$$

At very low values of κ, $\bar{\psi} \simeq \bar{\zeta} \simeq \kappa$ (approximation), the non-dimensional velocity and temperature profiles is converted to:

$$\bar{u} = \frac{3}{2}(1-\bar{y}^2) + \Gamma_2 \overline{E}_s \kappa(\bar{y}^2 - 1)$$

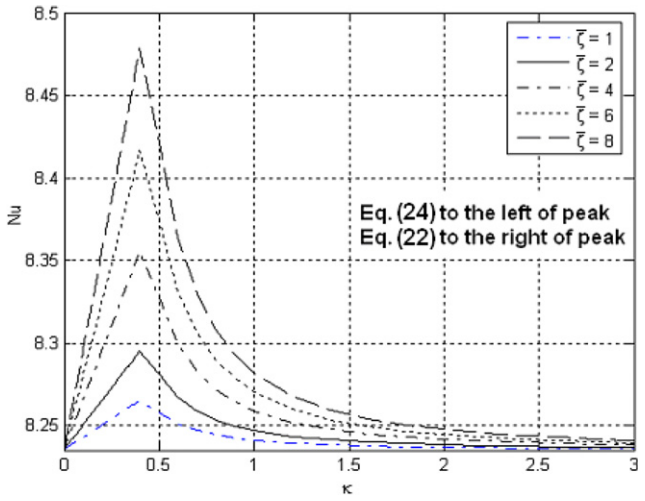

Fig. 4. Nusselt number variation at different non-dimensional zeta potential values.

and

$$\phi = \frac{Nu}{4}\left[\left(-\frac{\bar{y}^2}{2} + \frac{\bar{y}^4}{12} + \frac{5}{12}\right) + \Gamma_2 \overline{E}_s \kappa\left\{-\frac{\bar{y}^4}{12} + \frac{\bar{y}^2}{2} + \frac{1}{12} - \frac{1}{2}\right\}\right] \tag{24}$$

Solving for the Nusselt number, again we obtain Eq. (22), where I is now given by:

$$I = \int_{-1}^{1}\left[\frac{3}{2}(1-\bar{y}^2) + \Gamma_2 \bar{E}_s \kappa(y^2-1)\right]\left[\frac{3}{2}\left(-\frac{y^2}{2} + \frac{y^4}{12} + \frac{5}{12}\right) + \Gamma_2 \bar{E}_s \kappa\left\{-\frac{y^4}{12} + \frac{y^2}{2} + \frac{1}{12} - \frac{1}{2}\right\}\right] d\bar{y}$$

Plotting Nu for the complete range of values of κ, we get the results shown in Fig. 4.

The variation of Nusselt number with κ follows the same pattern as that of $C_f Re$ product. This is in correlation with Reynolds analogy also. However, unlike the effect for flow, the electrokinetic effects generally will be quite small on heat transfer.

3.4. Nusselt number – constant wall temperature

Using the energy balance equation for a small elemental area we get the following equation for the temperature profile:

$$\frac{d^2T}{dy^2} = \frac{u}{\alpha}\left(\frac{T - T_s}{T_m - T_s}\right)\frac{dT_m}{dx}$$

or

$$\frac{d^2T}{dy^2} = \frac{u}{\alpha}\left(\frac{T - T_s}{T_m - T_s}\right)\frac{q''}{\rho a U c_p}$$

In the non-dimensional form, the above equation can be rewritten as:

$$\frac{d^2\phi}{d\bar{y}^2} = -\frac{Nu}{4}(\bar{u})(\phi) \tag{25}$$

The Nusselt number for the constant wall temperature case is obtained from successive iterations of the basic non-dimensional temperature profile equation given by Eq. (25) by substituting the initial value of Nusselt number ($Nu = 8.235$) and the temperature profile for the constant heat flux condition (Eq. (23)) for infinite parallel plates.

Substituting successively the non-dimensional velocity and temperature profiles obtained from Eq. (25) and using the boundary conditions as:

At $\bar{y} = 0$, $\partial\phi/\partial\bar{y} = 0$ and at $\bar{y} = 1$, $\phi = 0$

we obtain the Nusselt number for the constant wall temperature condition. Using the temperature profiles obtained during the constant heat flux condition for different values of κ the Nusselt number variation with κ for constant temperature condition is the determined as shown in Fig. 5. The Nusselt number for constant temperature condition is obtained until the successive iteration of Eq. (25) yields the same value until 4 decimals of accuracy. Consistent

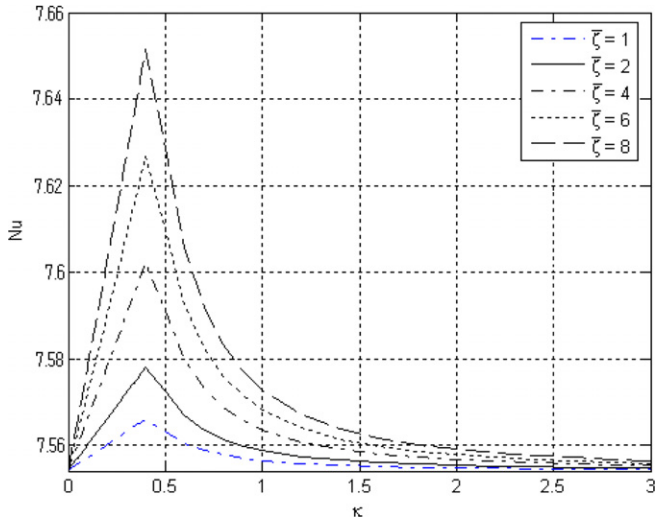

Fig. 5. Nusselt number variation with complete range of κ.

with the constant wall heat flux case, the effect of electrokinetics on heat transfer is quite small.

The electrolytic charge distribution and its movement near the wall is more for constant heat flux than constant temperature condition. This is because at constant temperature, the number density of the charges is fixed, whereas for constant heat flux the charge distribution varies continuously inducing motion near the wall, thereby enhancing heat transfer.

4. Conclusions

An analytical modeling of the effect of electrokinetics in microchannel fluid flow has been done. The concepts of EDL and zeta potential have been investigated in detail. It can be seen that on increasing the ionic strength of the fluid, the characteristic thickness of the EDL decreases.

Subsequently, using the Debye–Hückel linear approximation, the Navier–Stokes equation has been modified and the non-dimensional velocity profile has been developed, which clearly depicts that the presence of the EDL in the flow decreases the fluid velocity in the EDL regime. A heat transfer analysis is also done. An approximate approach was adopted to find appropriate $C_f Re$ and Nu results at lower values of κ. The primary conclusion is that electrokinetic effects can have a large effect on flow (for the right combinations of conditions), but the effect on heat transfer will be small.

References

[1] S. Wu, Microheat exchanger by using MEMS impinging jets, in: Proceedings of the 12th IEEE International Conference on MEMS, 1999, pp. 171–176.
[2] C.C. Wong, Development of a micro pump for microelectronic cooling, Int. Mech. Eng. Congr. Expos. (1996) 239–244.
[3] L.R. Arana, S.B. Schaevitz, A.J. Franz, M.A. Schmidt, K.F. Jensen, A micro fabricated suspended-tube chemical reactor for thermally efficient fuel processing, J. MEMS 12 (5) (2003) 600–612.
[4] D.L. Polla, MEMS technology for biomedical applications, in: Proceedings of 6th International Conference on Solid-State and Integrated Circuit Technology, vol. 1, 2001, pp. 19–22.
[5] L. Zhang, J.M. Koo, L. Jiang, M. Asheghi, K.E. Goodson, J.G. Santiago, T.W. Kenny, Measurements and modeling of two-phase flow in microchannels with nearly constant heat flux boundary conditions, J. MEMS 11 (1) (2002) 12–16.
[6] G.E. Kendall, P. Griffith, A.E. Bergles, J.H. Lienhard, Small diameter effects on internal flow boiling, in: Proceedings of ASME, IMECE, New York, 2001.
[7] X.Y. Chen, K.C. Toh, J.C. Chai, C. Yang, Developing pressure-driven liquid flow in microchannels under electrokinetic effect, Int. J. Eng. Sci. 42 (5–6) (2003) 609–622.
[8] G.M. Mala, D. Li, D. Dale, Heat transfer and fluid flow in microchannels, Int. J. Heat Mass Transfer 40 (13) (1997) 3079–3088.
[9] C. Yang, D. Li, Electrokinetic effects on pressure driven liquid flows in rectangular microchannels, J. Colloid Interface Sci. 194 (1997) 95–107.
[10] C.Y. Soong, S.H. Wang, Theoretical analysis of electrokinetic flow in microchannels with asymmetric boundary conditions, in: Proceedings of the 7th International Conference on Structure Engineering, Taiwan, August 2004.
[11] L. Kulinsky, Y. Wang, M. Ferrari, Electroviscous effects in microchannels, in: SPIE Conference on Micro and Nanofabricated Structures and Devices for Biomedical Environmental Applications II, San Jose, CA, vol. 3606, 1999, pp. 158–168.
[12] I. Papautsky, J. Brazzle, T. Ameel, A.B. Frazier, Laminar fluid behavior in microchannels using micropolar fluid theory, in: Sensors and Actuators, Physical Proceedings of the 11th IEEE International Workshop on MEMS, Heidelberg, Germany, vol. 73, 1998, pp. 101–108.
[13] G.M. Mala, D. Li, C. Werner, H.J. Jacobasch, Y.B. Ning, Flow characteristics of water through a microchannel between two parallel plates with electrokinetic effects, Int. J. Heat Fluid Flow 18 (1997) 489–496.
[14] A.V. Delgado, Interfacial electrokinetics and electrophoresis, in: Surfactant Science Series, New York, 2002.
[15] A.T. Conlisk, The Debye–Hückel approximation: its use in describing electroosmotic flow in micro- and nano-channels, Electrophoresis 26 (10) (2005) 1896–1912.